Submitted to Bulletin of Earthquake Engineering

SIMPLIFIED ESTIMATION OF SEISMIC RISK FOR REINFORCED CONCRETE BUILDINGS WITH CONSIDERATION OF CORROSION OVER TIME*

Daniel Celarec[1], Dimitrios Vamvatsikos[2] and Matjaz Dolsek[1]
[1]University of Ljubljana, Slovenia
[2]University of Cyprus, Cyprus

Abstract. *Throughout the world, buildings are reaching the end of their design life and develop new pathologies that decrease their structural capacity. Usually the ageing process is neglected in seismic design or seismic risk assessment but may become important for older structures, especially, if they are intended to be in service even after they exceed their design life. Thus, a simplified methodology for seismic performance evaluation with consideration of capacity degradation over time is presented, based on an extension of the SAC/FEMA probabilistic framework for estimating mean annual frequencies of limit state exceedance. This is applied to an example of an older three-storey asymmetric reinforced concrete building, in which corrosion has just started to propagate. The seismic performance of the structure is assessed at several successive times and the instantaneous and overall seismic risk is estimated for the near collapse limit state. The structural capacity in terms of the maximum base shear and the maximum roof displacement is shown to decrease over time. Consequently, the time-averaged mean annual frequency of violating the near-collapse limit state increases for the corroded building by about 10% in comparison to the typical case where corrosion is neglected. However, it can be magnified by almost 40% if the near-collapse limit state is related to a brittle shear failure, since corrosion significantly affects transverse reinforcement, raising important questions on the seismic safety of the existing building stock.*

Keywords: seismic risk, capacity degradation, corrosion, reinforced concrete frame, performance-based earthquake engineering, static pushover.

1 INTRODUCTION

Structures are exposed to aggressive environmental conditions which may cause different types of structural damage. For example, wind, waves, corrosive environment, extreme temperatures and earthquakes are the influences that can impact many existing structures every day. Such environmental conditions can cause corrosion or material fatigue that may lead to the extensive deterioration of mechanical properties of structural elements. Consequently, the structural capacity degrades over time and considerable costs have to be incurred just to maintain the serviceability of a structure and to assure its resistance to the loads that it was designed for.

Driven by the frequent failures of bridge structures, the influence of corrosion on their traffic load capacity has been widely researched. There, the effects of ageing are more severe since the entire structure is exposed to the environment. Different studies (Val et al. 1998; Estes and Frangopol 2001) show that deterioration of capacity resulting from reinforcement corrosion could have a significant effect on both serviceability and ultimate limit state of

* This article is based on short paper presented at the COMPDYN 2009 Conference (Rhodes, Greece).

bridge structures, and thus, have to be properly considered in system reliability assessments. Until recently, most work has focused on the assessment of aseismic bridges, but the latest studies (Choe at al. 2009; Kumar et al. 2009) demonstrate that the effect of corrosion becomes even more meaningful if the bridges are subjected to the seismic load. Less has been done for buildings, especially to quantify their degrading performance under seismic loads (e.g. Berto at al. 2009). Thus, we propose to investigate the effect of environmental corrosion on the seismic behaviour of reinforced concrete (RC) buildings in performance-based earthquake engineering terms. This effort becomes especially significant for older RC structures designed and constructed in the 1950–1960 era that are nearing the end of their nominal design life. The fundamental understanding of the effect of weathering on our ageing infrastructure will help us actually understand the performance of the structures during their entire life, not just when they are still intact.

The corrosion of reinforcement, which arises from carbonation phenomena and chloride-induced penetration, is one of the most important sources of deterioration for RC members (Val and Stewart 2009). The deterioration process related to the corrosion of reinforcement in general comprises two parts, that is, the corrosion initiation and corrosion propagation. The corrosion initiation is the process of diffusion and direct ingress of aggressive agents (e.g. chloride or carbon dioxide) through protective cover and cracks, while the corrosion propagation, which starts when the concentration of those agents at bar surface exceeds a threshold level, is related to formation of different damage in structural elements, such as loss of cross-sectional area of reinforcing steel, reduction of ductility and mechanical properties of reinforcing, reduction of bond and crack propagation like spalling and delamination of concrete protective cover caused by extensive corrosion products (Val and Stewart 2009).

Although models that consider all of the above-mentioned phenomena do exist, they can be cumbersome. For the purposes of our study, several simplifications were made in order to provide a simple and efficient estimate of the influence of corrosion on the seismic risk of RC structures. Therefore, a uniform corrosion was adopted along the longitudinal and transverse reinforcement bars of exposed structural elements, a simple model compared to more accurate spatial non-homogeneous pitting corrosion (Stewart 2009). The concrete spalling and reduction of maximum bond stress between concrete and reinforcement (Berto at al. 2009) bar were not included in the model. In other words, corrosion only influences the diameter of the steel bar. Also, the evaluation of the time to corrosion initiation, which depends on a large number of parameters such as the composition of concrete, its porosity and microstructure, the degree of pore saturation and the exposure conditions (Val and Stewart 2009), was not considered; we are focusing on an existing structure in which the corrosion process has just started to propagate. Therefore, the seismic risk was estimated for a time period of 50 years, starting from the initiation of corrosion in the structure. Such a simplified approach can be used for estimating the seismic risk in existing structures, which are expected to be in service well beyond the time that corrosion has set in, as typically happens when they exceed the lifetime that they were designed for.

Based on these simplifying assumptions, it would be attractive to use a closed-form expression to evaluate the performance of an ageing structure in terms compatible with current performance-based earthquake engineering concepts, i.e. in terms of the mean annual frequency (MAF) of exceeding a given limit state. One candidate is the engineering demand parameter (EDP) based methodology introduced by Torres and Ruiz (2007) that will be used for structural reliability evaluation in combination with the simplified seismic performance assessment method (Fajfar 2000; Dolšek and Fajfar 2007; Dolšek and Fajfar 2008). It is based on the SAC/FEMA probabilistic framework proposed by Cornell et al. (2002), in addition to which, the structural capacity is considered to change in time. Similarly, an intensity measure

(IM) based formulation is also considered as an alternative (Vamvatsikos and Dolšek, 2009). Both are able to provide an expected number of limit-state exceedance events and the overall time-averaged MAF over the period of interest that can be compared to typical acceptable rates of exceedance, e.g. the ubiquitous 2% or 10% in 50 years.

In the following sections, the proposed methodology is applied to an existing three-storey asymmetric non-ductile RC frame building. Our aim is to walk the reader through all the steps of a practical application on a realistic structure, taking shortcuts and making simplifications where appropriate to derive a basic result that can help us determine whether corrosion is worth considering when estimating the seismic performance of a given structure. Let us begin by briefly summarising the probabilistic framework.

2 SUMMARY OF PROBABILISTIC FRAMEWORK

Existing methods for structural performance assessment, such as that proposed by Cornell et al. (2002), are usually based on the estimation of the mean annual frequency (MAF) of violating the designated limit states or performance goals, where the resulting MAFs are assumed to remain constant throughout the design life of the structure. The MAF of exceedance of predefined limit states during any given time interval is then equal to the instantaneous MAF at any time. However, this cannot be the case under severe weathering conditions, where significant capacity degradation is expected to take a place and as a consequence the MAF increases with time. Thus, additional effort has to be done to account for capacity degradation over time.

Since the numerical evaluation of the time integral adds another layer of complexity, simplified methods for structural reliability evaluation considering the capacity degradation over time have recently been developed. In the present study we primarily use the reliability framework introduced by Torres and Ruiz (2007). Their method is a straightforward extension of the probabilistic framework proposed by Cornell et al. (2002), with the added assumption that the structural capacity $C\ \tau$ is a random variable with a probability density function $f_C\ c|\tau$, which changes with time. Therefore the conditional probability of failure $P\left[C\ \tau < D|y,\tau\right]$ is also a function of time and the expected number of limit state exceedance events within the time interval $t_0, t_0+\Delta t$ can be expressed as:

$$E\left[\eta\ t_0,\Delta t\ \right]=\int_{t_0}^{t_0+\Delta t}\int_0^{\infty}\int_0^{\infty}\left|\frac{dH(y)}{dy}\right|P\left[C\ \tau < D|y,\tau\right]f_C\ c|\tau\ dy\,dc\,d\tau\,. \qquad (1)$$

The variables of Eq.(1) are explained in more detail elsewhere (Torres and Ruiz 2007). The analytical solution of Eq. (1) provides two different formulations, which were both used in our study, that is, the Engineering Demand Parameter (EDP) based formulation and the Intensity Measure (IM) based formulation, which differentiate on how the seismic demands (*D*) and structural capacities (*C*) are defined. The formulations are explained in more detail in the following sections.

2.1 The EDP based formulation

The EDP based formulation, proposed by Torres and Ruiz (2007), is based on the engineering demand parameter, i.e. a measure of the structural response. In that case,Eq. (1) can be expressed in closed form, similarly as derived by Cornell et al. (2002). The expected number of limit state exceedance events η_{edp} over the time interval $t_0, t_0+\Delta t$ and the average MAF $\lambda_{\text{edp}}^{\text{AVG}}$ can then be written as:

$$\eta_{\text{edp}}\ t_0,\Delta t\ = H\ \hat{a}^0_{\text{g,ls}}\ \times\exp\left[\frac{k^2}{2\cdot b^2}\ \beta^2_{\text{DR}}+\beta^2_{\text{CR}}+\beta^2_{\text{DU}}+\beta^2_{\text{CU}}\ \right]\times\Omega\ t_0,\Delta t\ ,\ \lambda^{\text{AVG}}_{\text{edp}}=\frac{\eta_{\text{edp}}}{\Delta t},\quad (2)$$

where $H(\cdot)$ is the mean seismic hazard function, k_0 and k are the parameters of the power-law approximation to the hazard curve, β_{DR} is the dispersion measure for aleatory randomness in displacement demand, β_{CR} is the dispersion measure for aleatory randomness in displacement capacity, β_{DU} and β_{CU} are, respectively, the dispersion measures for epistemic uncertainty in displacement demand and capacity, and b is the exponent of the approximate power-law relationship between the IM and EDP. $\hat{a}^0_{\text{g,ls}}$ is the seismic intensity measure, in our case the peak ground acceleration, related to the median of the limit state capacity $\hat{C}\ t_0$ at the beginning of the evaluation time interval (t_0, $t_0+\Delta t$), and Ω is a derived parameter covering the specified time interval:

$$\hat{a}^0_{\text{g,ls}}=\left(\frac{\hat{C}\ t_0}{a}\right)^{\frac{1}{\text{b}}} \quad (3)$$

$$\Omega\ t_0,\Delta t\ =\frac{\alpha+\beta\cdot t_0}{\beta}\frac{b}{(b-k)}\left[\left(1+\frac{\beta\cdot\Delta t}{\alpha+\beta\cdot t_0}\right)^{1-\frac{k}{b}}-1\right]. \quad (4)$$

The simplified approach presented above is based on several assumptions. The hazard curve has to be approximated considering an appropriate interval around $\hat{a}^0_{\text{g,ls}}$, and the relationship between the IM and the EDP has to be fitted around the $\hat{C}\ t_0$, both accomplished by the following power-law expressions:

$$H\ \hat{a}_g\ =k_0\cdot\hat{a}_g{}^{-\text{k}},\ \hat{D}\ t\ =a\cdot\hat{a}_g{}^{\text{b}}. \quad (5)$$

Additionally, the median capacity $\hat{C}\ t$ is assumed to vary linearly with time:

$$\hat{C}\ t\ =\alpha+\beta\cdot\Delta t,\ \alpha>0 \text{ and } \beta\leq 0, \quad (6)$$

where α in β are the parameters defining the linear function (note, that parameter β without subscripts has no relation with those defining dispersion measures in Eq. (2)). It is also assumed that all dispersion measures and the parameters of the relationship between the IM and the EDP (a, b) are constant over the integration time interval Δt. The demand D(t) and capacity C(t) are assumed to be lognormally distributed. The dispersion measures related to demand and capacity are therefore defined as the standard deviation of the logarithm of the demand and capacity, respectively.

2.2 The IM based formulation

Unlike the case of the EDP formulation, the IM based approach (e.g. Cornell et al. 2002) requires structural capacity expressed in terms of the earthquake intensity measure, which can be for example, the spectral acceleration S_{a} or the peak ground acceleration a_{g}. This alternative formulation has several theoretical advantages compared to the standard EDP-based formulation. For example, an approximation of the relationship between the seismic intensity measure and engineering demand parameter is not needed, and the IM based formulation also does not require any correlation assumptions between demand and capacity.

Starting again from Eq. (1) and using similar assumptions to those presented earlier, (Vamvatsikos and Dolšek 2009) have derived the expression for the expected number of limit

state exceedance events η_{edp} over the time interval (t_0, $t_0+\Delta t$) and the average MAF λ_{im}^{AVG} as follows:

$$\eta_{im}\left(t_0,\Delta t\right)=k_0\left(\hat{a}_{g,ls}^{0}\right)^{-k}\cdot\exp\left[\frac{k^2}{2}\left(\beta_{Rag}^2+\beta_{Uag}^2\right)\right]\cdot\frac{\hat{a}_{g,ls}^{0}}{\gamma\cdot(1-k)}\left[\left(1+\frac{\gamma\cdot\Delta t}{\hat{a}_{g,ls}^{0}}\right)^{1-k}-1\right],\ \lambda_{im}^{AVG}=\frac{\eta_{im}}{\Delta t} \quad (7)$$

where β_{Rag} and β_{Uag} are the dispersion measures in intensity measure for randomness and uncertainty, k_0 and k are the parameters of the hazard curve approximation, and $\hat{a}_{g,ls}^{0}$ is the median peak ground acceleration corresponding to the predefined limit state (e.g. near collapse limit state). Note that parameters $\hat{a}_{g,ls}^{0}$ of the Eq. (2) and Eq. (7) are in general different, since in the first case the $\hat{a}_{g,ls}^{0}$ is determined indirectly through EDP-capacity whereas in the later case it is determined directly through IM-capacity.

Expression (7) was derived considering the assumption that structural capacity $\hat{C}(t)$ varies linearly in time. For mathematical convenience it was assumed that value of that linear function at time t_0 corresponds to the structural capacity at the same time, which is a further simplification compared to the Torres and Ruiz (2007) formulation. Thus, the linear function of structural capacity $\hat{C}\ t$ is defined with a single parameter γ only:

$$\hat{C}\ t\ =\hat{C}\ t_0\ +\gamma\cdot\Delta t,\ \gamma\leq 0, \quad (8)$$

where γ defines the slope of the linear function.

2.3 Simplified method for seismic performance assessment of structures

Determination of the relationship between the seismic intensity measure and the engineering demand parameter may become extremely time-consuming. This is especially the case if the structural response is estimated with nonlinear dynamic analysis, which, even for a single instant in the building's lifetime, has to be performed for several intensity measures and different ground motion records, e.g. with incremental dynamic analysis (IDA) (Vamvatsikos and Cornell 2002), in order to capture randomness due to earthquakes. In addition, analyses will have to be performed for different times within the lifetime of interest to capture the effect of corrosion. Therefore, for practical application, simplified analysis methods become very attractive. In our study, the time-dependent relationship between the seismic intensity measure and the engineering demand parameter was determined with the incremental N2 analysis (IN2) (Fajfar 2000; Dolšek and Fajfar 2007). It is a simplified nonlinear method for seismic performance assessment of structures and represents an alternative to IDA (Vamvatsikos and Cornell 2002).

The procedure for determination of the IN2 curve is explained elsewhere (Dolšek and Fajfar 2007). For common structural systems with moderate or long fundamental period(s) the IN2 curve results in a straight line. In this case the "equal displacement rule" applies, i.e. b=1.0 (Eq. (5)), up to the "failure" point, which is conservatively represented by the near collapse limit state. After "failure", the IN2 curve becomes a horizontal line. In more general cases, the IN2 curve can be approximated in the same way as a mean IDA curve, i.e. from two points of the actual curve, e.g. from the points representing the damage limitation and near collapse limit states, or by regression over several discrete points.

Since the IN2 curve is only a "central" (mean or approximately median) result, it does not contain any dispersion information. Therefore the dispersion values for randomness in displacement demand β_{DR} and displacement capacity β_{CR} cannot be determined. A possible alternative is using SPO2IDA instead, a simple-to-use tool that employs complex R-μ-T relationships to provide the median and the 16, 84 percentiles of demand or capacity

(Vamvatsikos and Cornell 2006). This allows the estimation of both the needed median dispersion of capacity for complex pushover shapes and will provide accurate results. Alternatively, they can be estimated directly by performing IDA for the equivalent SDOF system as also shown in Dolšek and Fajfar (2007). Still, our pushover shapes are practically elasto-plastic, allowing the use of existing results from other works, (e.g. Dolšek and Fajfar 2007; Ruiz-Garzia and Miranda 2003), who have found that the coefficient of variation for the displacement of such SDOF systems varied from 0.4 for structures with a moderate or long natural period, to 0.7 for structures with a short predominant period. The determination of dispersion measures for uncertainty in displacement demand β_{DU} and capacity β_{CU} is in general possible to determine with the IN2 method, but requires a probabilistic structural model, i.e. a model with appropriate consideration of parameter uncertainties, which is not within the scope of this paper. For a simplified approach, it is convenient to predetermine the dispersion measures for uncertainty. For example, dispersions for steel frames have been proposed in the FEMA-350 Guidelines (2000). They may serve as rough estimates also for some other structural systems. For example, the total uncertainty dispersion measure $\beta_{\mathrm{UT}} = (\beta_{\mathrm{DU}}^2 + \beta_{\mathrm{CU}}^2)^{0.5} = 0.35$ was applied for a global inter-story drift evaluation in the case of low-rise buildings within the SAC/FEMA seismic performance evaluation (Yun et al. 2002). The dispersions in intensity measure due to randomness and modelling uncertainties for different types of structural systems and for the IM based approach were recently proposed in FEMA P695 (2009). The values for record-to-record and modelling-related variability are in range of 0.35 to 0.45 for randomness and 0.2 to 0.65 for uncertainties.

3 EXAMPLE OF THE THREE-STOREY RC FRAME BUILDING

As an example of our methodology, we will estimate the seismic risk for an existing frame building, in which the reinforcement corrosion has just initiated. The structure is located in a region of moderate seismic hazard and high level of reinforcement corrosion risk area, a typical scenario for most coastal areas in the Mediterranean. The objective of the analysis is to estimate the increase in seismic risk for two predefined near-collapse limit states as the associated structural capacity degrades with time.

The structure was analysed at different time instants (t_0+Δt), in which t_0 relates to the initial condition of the existing structure, when corrosion attack was detected, and Δt is the time interval during which the propagation of corrosion is taking place. Since the evaluation interval is taken to be [0, 50yrs], t_0 was set to zero in Eq. (2), (4) and (8). For the discussions to follow, the term "initial structure" will relate to the structure at time t_0, at which it was assumed that reinforcement corrosion did not affect the structural capacity yet, and the term "degraded structure" will relate to the structure affected by corrosion at selected time instants Δt.

3.1 Description of the structure and model

The example structure is a three-storey asymmetric reinforced concrete frame building. This structure was pseudo-dynamically tested within the European research project SPEAR (Seismic performance assessment and rehabilitation of existing buildings, M. Fardis and P. Negro, coordinators) and analysed in previous studies (e.g. Fajfar et al. 2003). The elevation, the plan of the building and the reinforcement of typical cross sections of the columns and beams are shown in Figure 1. The structure was designed for gravity loads only.

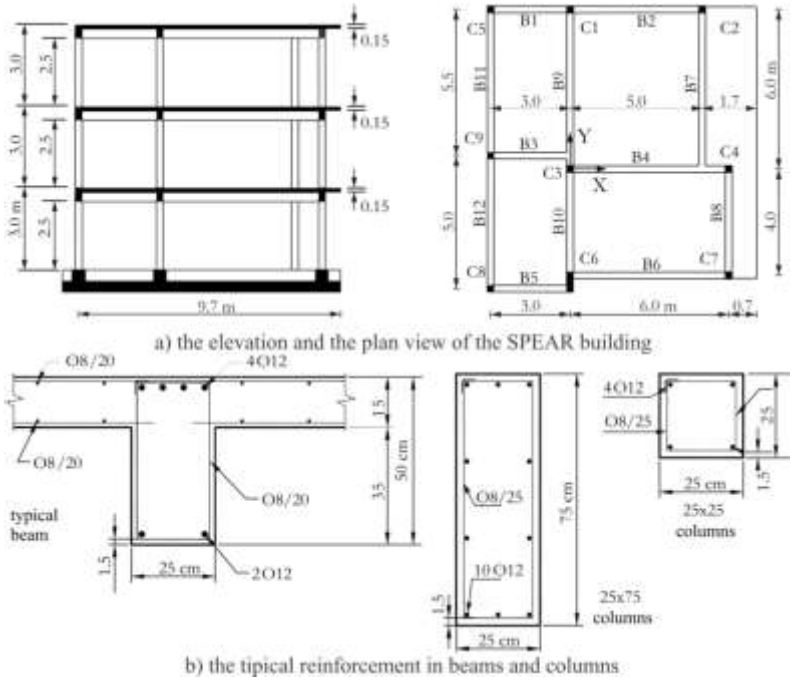

Figure 1: a) The elevation and plan view of example structure, and b) typical cross-sections and reinforcement in columns and beams.

The columns and beams of the structure were modelled by one-component lumped plasticity elements, which consist of an elastic beam-column element and two inelastic rotational hinges at the ends, defined by a moment-rotation relationship. These relationships were determined for the columns by properly taking into account their axial load and its interaction with the moment capacity. Gravity loads for this RC structure amounted to 6.3 kN/m^2 and 6.2 kN/m^2 for first two stories and top storey, respectively.

Rigid diaphragms were assumed at the floor levels due to monolithic RC slabs. Consequently the masses were lumped at the mass centres. The lumped masses and the corresponding mass moments of inertia amounted to 65.5 t and 1196 tm^2 for the first two stories, and 64.1 t and 1254 tm^2 for the top storey, respectively. The centreline dimensions of the elements were used with the exception of beams which are connected eccentrically to the column C6. Using centreline dimensions, the storey heights of 2.75 and 3.0 m, respectively, for the first and upper two storeys, were assumed.

A schematic moment-rotation relationship is shown in Figure 2. The yield (M_y) and maximum moment (M_m) was determined from appropriate section analysis. The characteristic rotations, which describe the moment-rotation envelope of a plastic hinge, were determined according to the procedure described by Fajfar et al. (2006). The zero moment point was assumed to be at the mid-span of the columns and beams. Therefore the rotations θ_y for moment-rotation envelopes of columns and beams were calculated using the formula:

$$\theta_y = \frac{M_y \cdot l_{span}}{6 \cdot E \cdot I_{eff}}, \tag{8}$$

where l_{span} is the length of a beam or column, E is the modulus of elasticity and I_{eff} is the effective moment of inertia of the element (0.5 I).

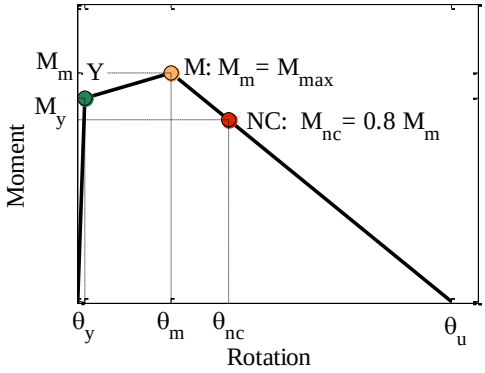

Figure 2: Schematic moment-rotation relationship of a plastic hinge in columns and beams.

The near collapse rotation $\theta_{nc,c}$ in the columns, which corresponds to a 20 % reduction in the maximum moment, was estimated by means of the Conditional Average Estimator (CAE) method (Perus et al. 2006), whereas the near collapse rotation for hinges in beams $\theta_{nc,b}$ were determined using the formula defined in Eurocode 8 (2005):

$$\theta_{nc,b} = \frac{1}{\gamma_{el}} 0.016 \cdot (0.3^{\nu}) \cdot \left[\frac{\max(0.01;\omega')}{\max(0.01;\omega)} f_c \right]^{0.225} \cdot \left(\frac{L_V}{h} \right)^{0.35} \cdot 25^{\left(\alpha \rho_{sx} \frac{f_{yw}}{f_c} \right)} \cdot (1.25^{100\rho_d}). \qquad (9)$$

where γ_{el} is equal to 1.0 (mean values), parameter ν is the normalised axial load (for beams: ν=0), ω and ω' are the mechanical reinforcement ratios of the tension and compression longitudinal reinforcement, respectively, f_{cm} and f_{yw} are the mean strength of concrete (MPa) and yield strength of steel (MPa), respectively, ρ_{sx} is the ratio of transverse steel parallel to the direction of loading, ρ_d is the steel ratio of diagonal reinforcement in each diagonal direction and α is the confinement effectiveness factor. All beams are defined as members without detailing for earthquake resistance. Therefore the rotations at near collapse limit state $\theta_{nc,b}$ are multiplied by 0.825. The post-capping or negative-stiffness part of moment-rotation envelope is determined under the assumption that the ratio between the ultimate rotation $\theta_{u,b}$ and rotation at maximum moment $\theta_{m,b}$ is 3.5.

The degradation of capacity over time was modelled only via the simplified model of corrosion of longitudinal and transverse reinforcement in the external (i.e. exposed) elements of the structure. In general, the corrosion decreases the diameter of reinforcement and the bond stress between the concrete and steel bars. The later phenomenon and as well as spalling of concrete were not considered in this stage of the study. Therefore in our model the corrosion influences only the diameter of the steel bar. The reduced diameter $D_{rb}(t)$ of a reinforcing steel bar with initial diameter of D_b (mm), which is subjected to corrosion for a time period (years) $\Delta t = t - t_0$ (t_0 relates to the initial condition of the building and is equal to 0) is, according to Pantazopolou and Papoulia (2001):

$$D_{rb} = D_b - 0,023 \cdot i_{corr} \cdot \Delta t, \qquad (10)$$

where i_{corr} represent the mean annual corrosion current per unit anodic surface area of steel ($\mu A/cm^2$). In our analysis the corrosion current i_{corr}=1.2 $\mu A/cm^2$ was considered, which corresponds to a high level of reinforcement corrosion (Pantazopolou and Papoulia 2001).

In order to determine the structural capacity as a function of time, six structural models M_0, M_{10}, M_{20}, M_{30}, M_{40} and M_{50} were prepared on the OpenSees platform (McKenna and Fenves 2004) in combination with the PBEE toolbox (Dolsek 2009). These correspond to the initial condition of the building at time t_0=0 and to the degraded structure (affected by corrosion) after 10, 20, 30, 40 and 50 years of corrosion propagation, respectively. The first three modal

periods of the initial 3D structure are: T_1=0.80 s T_2=0.67 s and T_3=0.538 s and are changing with time as the corrosion reduces the capacity. The period T_2 and the associated mode shape actually correspond to the first translational mode in the Y direction, which is the most critical for the seismic performance of the structure. Therefore the second mode shape will be exclusively used for applying the N2 method.

3.2 Definition of the limit states and nonlinear static analyses

The MAF of exceedance was determined for a near collapse limit state and for additional limit state which is related to the potential brittle failure and defined by a storey shear demand/capacity ratio (DCR) equals 0.5. The reason for such a definition of the second limit state is described later on in this Section.

According to European standard Eurocode 8 (2005) the near collapse (NC) limit state at the element level is defined with the ultimate rotation θ_{nc}, which corresponds to 20% drop of moment in the softening range of the moment-rotation relationship (Figure 2), and it is related to a ductile collapse mechanism. The NC limit state can also be defined on the basis of the shear strength, which is related to a brittle collapse mechanism. In this case the shear strength (capacity) of an element was calculated according to Eurocode 8 (2005):

$$V_R = \frac{1}{\gamma_{el}}\left[\frac{h-x}{2L_V}\min\ \{N; 0,55A_c f_c\} + 1 - 0,05\min\ \{5; \mu_\Delta^{pl}\}\right]\cdot \left[0,16\max\ \{0,5; 100\rho_{TOT}\}\left(1 - 0,16\min\left(5; \frac{L_V}{h}\right)\right)\sqrt{f_c}A_c + V_W\right], \tag{11}$$

where γ_{el} was assumed 1.0 in order to get the mean value of the shear strength, h is the depth of cross-section, x is the height of compressive zone, L_v is the moment-shear ratio (M/V), A_c is the cross-section area calculated as $b_w \cdot d$, f_c is the concrete compressive strength, ρ_{tot} is the total longitudinal reinforcement ratio and V_w is the contribution of transverse reinforcement to shear resistance, taken as equal to:

$$V_w = \rho_w \cdot b_w \cdot z \cdot f_{yw}, \tag{12}$$

where ρ_w is the transverse reinforcement ration, b_w is the width of the rectangular web of the cross-section, z is the length of the internal lever arm and f_{yw} is the yield stress of the transverse reinforcement.

Since the limit state at the building level is not defined in the European standard it was simply assumed that the near collapse limit state appears whether the base shear strength of structure, in relation to its static pushover curve, reduces to 20% of its maximum value, or the storey shear demand/capacity ratio (DCR) at any storey is equal or exceeds 1. Such definition is needed since the elastic model of shear was used in the analysis. In this place it is worth to emphasize that the structure under investigation is not sensitive to a brittle failure (shear DCR never exceeds 1) although corrosion significantly affects transverse reinforcement. However, we wanted to show how much the reduction of transverse reinforcement due to corrosion affects the MAF of violating the potential brittle limit state. Therefore, the MAF was estimated for an additional limit state (i.e. a potential brittle limit state), which is defined by a storey shear demand/capacity ratio (DCR) at any storey equals 0.5. Note that this limit state limit state is not related to near collapse limit state, but is a good indicator of the effect of corrosion on a potential shear failure.

In general, nonlinear static analysis is performed independently in the X and Y direction. For brevity, results are presented only for pushover analysis in the Y direction of the global coordinate system that is in the positive direction of the strong side of column C6 (Figure 1). The influence of the unsymmetrical plan of the structure on the results of the analyses is practically negligible. The imposed horizontal loads were determined by the product of storey masses and modal shape (Fajfar 2000), and are presented later in Section 3.3. The displacement of the structure was monitored at the mass centre at the roof.

The nonlinear static (pushover) analyses were performed for six structural models (M_0, M_{10},…, M_{50}), starting with the conditions of the initial structure, and then simulating structural response after every 10 years, to provide the capacity of the structure as a function of time. The results of the nonlinear static analysis (pushover curves) are presented in Figure 3. The values for the maximum load resistance F_{max} and the associated displacements D_{nc} and D_{pb}, which correspond to the NC limit state and potential brittle limit state, are presented in Table 1.

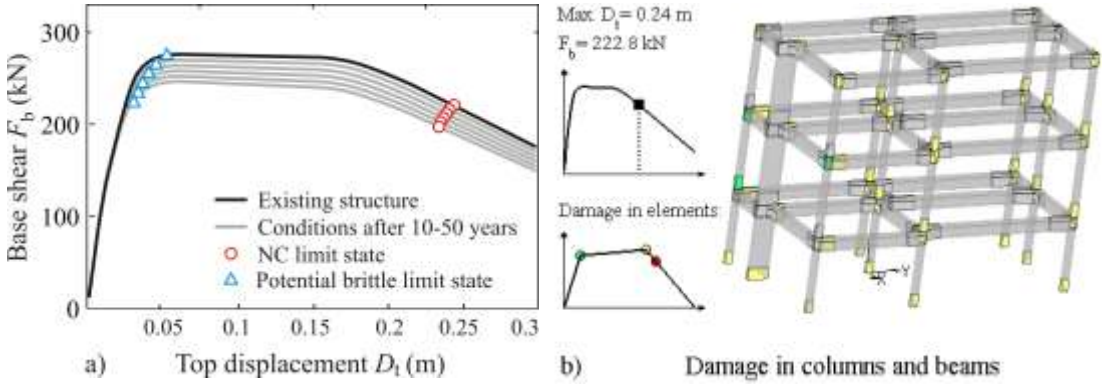

Figure 3: a) the pushover curves for different time instants and the points indicating the NC and potential brittle limit state and b) the damage in columns and beams at NC limit state for initial condition (t_0).

The base shear strength versus weight ratio starts at 14% for the initial structure and decreases with age under the influence of the corrosion. After 50 years of corrosion propagation the strength of the structure is reduced by about 11%. The difference in the roof displacement in the NC limit state due to ageing of the structure is not as important as the difference in the strength of the structure as it only amounts to 3.7%. The reason is that area of the longitudinal reinforcement does not have an important influence on the ultimate rotation in plastic hinges (Figure 3). On the other hand the roof displacement that corresponds to the potential brittle limit state is significantly reduced by about 42%.

Table 1: The values for the maximum base shear F_{max} and the roof displacements corresponding to the NC and potential brittle limit state.

Condition	Time instant Δt (y)	Max. load F_{max} (kN)	NC limit state D_{nc} (m)	Potential brittle limit state D_{pb} (m)
Initial	0	278	0.244	0.053
Corroded	10	272	0.242	0.046
	20	266	0.240	0.041
	30	260	0.238	0.037
	40	254	0.236	0.034
	50	248	0.235	0.031
$(F_{max,50} - F_{max,0}) / F_{max,0}$		-10.8 %	-	-
* $(D_{ls,50} - D_{ls,0}) / D_{ls,0}$		-	-3.69 %	-42%

* D_{ls} corresponds to the displacements at NC or potential brittle limit state.

3.3 Seismic capacity at different time instants

The definition of the structural capacity as a function of time differs depending on the probabilistic formulation. The EDP based formulation requires the structural capacity expressed in terms of an appropriate engineering demand parameter, whereas the IM based formulation depends on the structural capacity being expressed via the intensity measure, e.g. peak ground acceleration or spectral acceleration.

In the case of the EDP-based formulation, the structural capacity is defined in terms of the maximum roof displacement that corresponds to the predefined limit states, whereas for the IM-based formulation, the structural capacity is defined with the lowest peak ground acceleration that causes violation of each limit state. The relation between the maximum roof displacement and the peak ground acceleration is computed with the N2 method (Fajfar 2000) for the seismic load, which is defined with the elastic response spectrum according to Eurocode 8 (2004) for soil class C (S=1.15, T_C=0.6 s).

The roof displacements that correspond to the separate limit states were already reported in Section 3.2. In this Section determination of peak ground acceleration capacity $a_{g,nc}$ is explicitly demonstrated only for the NC limit state and for the initial building condition, i.e. for model M_0, while for degraded structures and for the potential brittle limit state only the final results are presented.

Once the results of pushover analysis are available, the pushover curve has to be idealized as shown in Figure 4a in order to determine the properties of the equivalent single degree of freedom (SDOF) model. The results of this idealization are the yield force F_y and yield displacement D_y. The properties of the SDOF system are then determined by dividing the corresponding properties of the MDOF system by the transformation factor Γ:

$$\Gamma = \frac{m_{SDOF}}{\sum m_i \cdot \phi_i^2} = 1.27;\ m_{SDOF} = \sum m_i \cdot \phi_i = 128.6 \text{ t}, \tag{2}$$

where m_{SDOF} is the mass of SDOF system, m={65.6, 65.6, 64.1} t is a vector of storey masses, and ϕ_Y={0.28, 0.70, 1.00} is the mode shape vector (normalized by its roof component) of the predominant translational mode shape in the Y direction, which in our example corresponds to T_2=0.67 s. The yield point of the equivalent SDOF system is obtained simply as $d_y^* = D_y/\Gamma = 0.025$ m and $f_y^* = F_y/\Gamma = 220$ kN. The period of the SDOF system is calculated as follows:

$$T_{SDOF} = 2 \cdot \pi \cdot \sqrt{\frac{m_{SDOF} \cdot d_y^*}{f_y^*}} = 0.753 \text{ s}. \tag{13}$$

The periods of all equivalent SDOF systems over all building ages are obviously within the medium-period range of the spectrum (Figure 4) and exceed the characteristic period T_C, which is the corner period between the constant acceleration and constant velocity ranges in an idealized Newmark-Hall type spectrum. Therefore, the equal displacement rule can be applied for the determination of the mean (or approximately median) spectral acceleration, which corresponds to the NC limit state. Therefore the $S_{ae,nc}$ is:

$$S_{ae,nc} = d_{nc}^* \cdot \left(\frac{2 \cdot \pi}{T_{SDOF}} \right)^2 = 13.4 \text{ m/s}^2 \tag{14}$$

where $d_{nc}^{*} = D_{nc}/\Gamma$, and the mean/median peak acceleration $a_{g,nc}$ corresponding to the NC limit state is determined from the elastic spectrum as follows:

$$a_{g,nc} = \frac{S_{ae,nc}\ T_{SDOF}}{S \cdot \eta \cdot 2.5} \cdot \frac{T_{SDOF}}{T_C} = 5.87\ \text{m/s}^2 = 0.598\ \text{g}. \quad (15)$$

The above evaluation of the $a_{g,nc}$ can be presented in the acceleration-displacement (AD) format together with the capacity diagram of the SDOF system (Figure 4b).

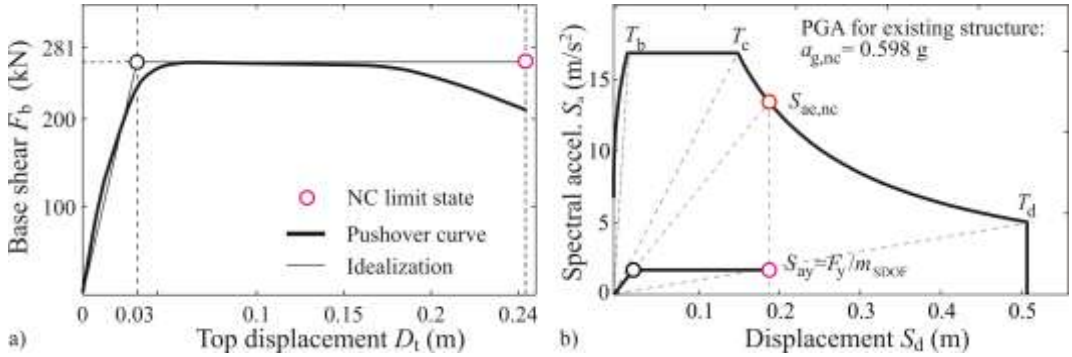

Figure 4: a) Idealization of the pushover curve for model M_0 and b) the AD format for the equivalent SDOF system.

This procedure was repeated to evaluate the peak ground acceleration capacity that corresponds to the NC and potential brittle limit states and for all degraded structures (models M_{10} to M_{50}). The resulting peak ground acceleration capacities $a_{g,nc}$ and $a_{g,pb}$ are presented in Table 2. The reduction in peak ground acceleration capacities for both limit states is similar to that shown before for the maximum roof displacement (Section 3.2, Table 1) and is about 4.5% for the NC limit state and 40% for the potential brittle limit state.

Table 2: The peak ground acceleration capacities $a_{g,nc}$ and $a_{g,pb}$ for the NC and potential brittle limit states.

Condition	Time instant Δt (y)	NC limit state $a_{g,nc}$ (g)	Potential brittle limit state $a_{g,pb}$ (g)
Initial	0	0.598	0.131
Corroded	10	0.592	0.114
	20	0.586	0.103
	30	0.581	0.093
	40	0.575	0.086
	50	0.571	0.079
*$(a_{g,ls,50} - a_{g,ls,0}) / a_{g,nc,0}$		- 4.5 %	-40 %

*$a_{g,ls}$ corresponds to the peak ground acceleration capacities for NC or potential brittle limit state.

The results presented in Table 2 are used as input data for the definition of the seismic capacity as an approximately linear function of time (Eq. (2) and (7)). The parameters α, β and γ that approximate the capacity as a linear function were calculated using linear regression (i.e. the method of least squares) for the EDP and IM-based format. The results are presented in Table 3. The roof displacements corresponding to each limit state defined at each time instant are presented in Figure 5. The fitted lines approximate the linear decrease of the median capacity with time after corrosion initiation.

Table 3: The parameters defining the linear functions for structural capacity in time.

Formulation	Units	NC limit state	Potential brittle limit state
EDP-based	m, year	α=0.244 m, β=-1.86×10^{-4} m/y	α=0.051 m, β=-4.0×10^{-4} m/y
IM-based	g, year	γ=-5.60×10^{-4} g/y	γ=-1.1×10^{-3} g/y

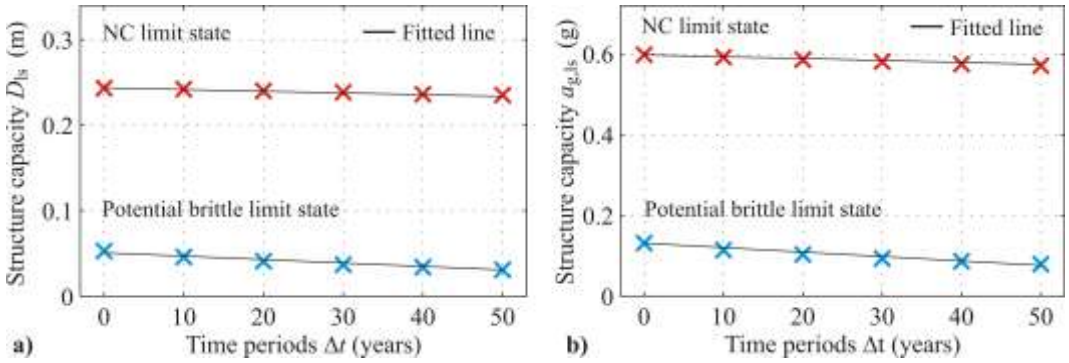

Figure 5: The values of maximum roof displacement and peak ground accelerations capacities ($a_{g,ls}$) at predefined building ages and their linear approximation for the NC and potential brittle limit state. The results are presented for a) EDP- and b) IM-based format, respectively.

3.4 Instantaneous and overall seismic risk

The expected number of exceedance events and average MAFs of the NC and potential brittle limit state were calculated by means of Eq. (2) and Eq. (7) for the initial conditions at time t_0=0, which corresponds to initial structure, and for different time periods, i.e. 10, 20, 30, 40 and 50 years.

The moderate seismic hazard typical for the South-East part of Slovenia (Dolšek and Fajfar 2008), was adopted in the procedure for the estimation of the seismic risk. This was approximated by a two-parameter seismic hazard function, derived separately for both limit states. The associated parameters k and k_0 were determined by locally fitting the hazard curve with the function $H(a_g)=k_0\cdot(a_g)^{-k}$ (Cornell et al. 2002). The fitting was performed over the interval from 0.25 $a_{g,ls}(t_0)$ to 1,25 $a_{g,ls}(t_{50})$ (Dolšek and Fajfar 2008), where $a_{g,ls}(t_0)$ is the median peak ground acceleration capacity of the initial structure for the selected limit state, and $a_{g,ls}(t_{50})$ is the corresponding capacity of the degraded structure after 50 years, that is, at the end of the considered time interval. Since $a_{g,ls}(t)$ differs for the NC and the potential brittle limit state, as marked on the curve on Figure 6, the parameters of the hazard curves also differ for both defined limit state, a fact that helps improve the accuracy of the closed form approximation in Cornell at al. (2002). The parameters are k=3.50, k_0=6.40×10^{-6} for the NC limit state and k=1.36, k_0=2.73×10^{-4} for the potential brittle limit state.

Note that parameter k need not be used in Eqs. (2) and (7) since the hazard corresponding to $a_{g,ls}(t)$ can be determined directly from the hazard curve. The seismic hazard curve used for peak ground acceleration is presented in Figure 6. The intensities for return periods 225, 475 and 2475 years are 0.293g, 0.181g and 0.325g, respectively, and the mean/median peak ground acceleration capacities derived from IN2 for the initial structure, are 0.530g and 0.121g for the NC and potential brittle limit state. As corrosion propagates, these will decrease with time.

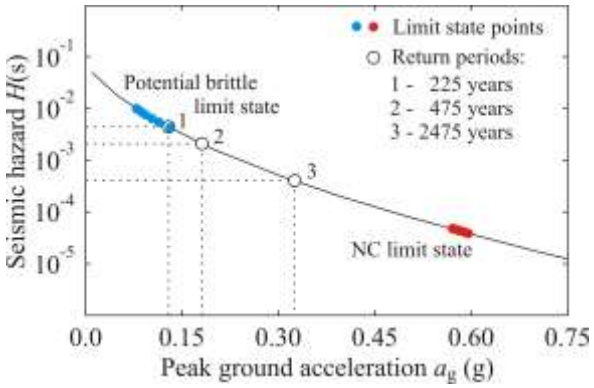

Figure 6: The seismic hazard curve and the median points for when the NC and the potential brittle limit state is achieved.

The dispersions for randomness in displacement demand and capacity were considered to be equal to 0.4 and 0.2, respectively, whereas the dispersions for uncertainty were considered to be the same for both the displacement demand and capacity and equal to 0.25. Unlike the EDP-based formulation, the IM format requires only the dispersion in intensity measure, which was assumed to be equal to 0.40 for both randomness and uncertainty.

The values for the expected number of exceedance events of the NC and potential brittle limit state at different times and the corresponding values of the average MAFs, using both the EDP and IM formulation, are collected in tables 4 and 5. The results are compared with the case, in which the degradation of structural capacity was neglected. In the latter case, the instantaneous MAFs of exceedance are all equal to the initial MAF at time t_0, and obviously equal to the time-average MAF as silently assumed in all typical performance-based earthquake engineering calculations.

The expected numbers of exceedance events for the potential brittle limit state per time interval of 50 years, using the EDP and IM based formulation, is estimated at 0.39 and 0.40, respectively, and it is about 39 and 43 % higher than the case in which the degradation was not considered. Note that it is assumed that the potential brittle limit state is detected when storey shear demand/capacity ratio at any storey equals to 0.5. On the other hand, the corrosion has only slightly influenced the moment capacity of the structural elements. Thus, the expected number of exceedance events for the NC limit state per time interval of 50 years is increased by only for 7.1 and 8.8 %, if considering the capacity degradation over time and amounts to 1.48×10^{-2} and 1.46×10^{-2}, depending on which formulation (EDP or IM) is used.

The results of the EDP-based formulation are also presented in Figure 7. The continuous curve represents the expected number of exceedance events for both limit states considering the capacity degradation over time and the dashed line represents the case when the degradation was neglected. The picture 7a and 7b are related to the NC and the potential brittle limit state, respectively.

Table 4: The expected number of exceedance events η_{edp} and the average MAFs λ_{edp}^{AVG} for the NC and potential brittle limit state using the EDP-based formulation.

Condition	Time interval	NC limit state		Potential brittle limit state	
	Δt (y)	$\eta_{edp}\left(\times 10^{-2}\right)$	$\lambda_{edp}^{AVG}\left(\times 10^{-4}\right)$	$\eta_{edp}\left(\times 10^{-2}\right)$	$\lambda_{edp}^{AVG}\left(\times 10^{-4}\right)$
No degradation	**50**	**1.38**	**2.77**	**27.9**	**5.59**
Corroded	10	0.28	2.80	5.91	5.91
	20	0.57	2.84	12.5	6.27
	30	0.86	2.88	20.1	6.69
	40	1.17	2.92	28.7	7.18
	50	**1.48**	**2.96**	**38.8**	**7.77**
*($x_{deg,50}$ - $x_{nodeg,50}$) / $x_{nodeg,50}$		+ 7.1 %	+ 7.1 %	+ 39 %	+ 39 %

*x corresponds to η or λ

Table 5: The expected number of exceedance events η_{im} and average MAFs λ_{im}^{AVG} for the NC and potential brittle limit state using the IM based formulation.

Condition	Time interval	NC limit state		Potential brittle limit state	
	Δt (y)	$\eta_{im}\left(\times 10^{-2}\right)$	$\lambda_{im}^{AVG}\left(\times 10^{-4}\right)$	$\eta_{im}\left(\times 10^{-2}\right)$	$\lambda_{im}^{AVG}\left(\times 10^{-4}\right)$
No degradation	**50**	**1.34**	**2.68**	**27.8**	**5.56**
Corroded	10	0.27	2.73	5.90	5.90
	20	0.55	2.77	12.6	6.30
	30	0.84	2.82	20.2	6.76
	40	1.14	2.87	29.3	7.30
	50	**1.46**	**2.92**	**39.8**	**7.97**
*($x_{deg,50}$ - $x_{nodeg,50}$) / $x_{nodeg,50}$		+ 8.8 %	+ 8.8 %	+ 43 %	+ 43 %

*x corresponds to η or λ

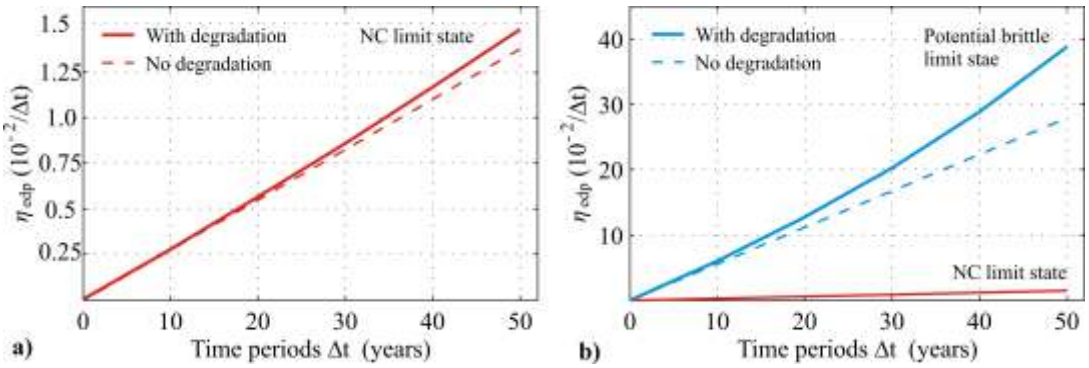

Figure 7: The expected number of exceedance events of (a) NC limit state and (b) potential brittle limit state using the EDP based methodology.

3.5 Discussion of the results

One important outcome of the study is the comparison between the EDP and IM-based formulations. The difference in the results amounts to 2 % and 10 % for NC and potential brittle limit state, respectively, and it is practically negligible. Basically, the only sources of difference are the values of the dispersion measures, which in our case were assumed as average values of the reported dispersions from the literature. All other parameters (see Eqs. (2) and (7)) practically do not contribute to the differences in the final results obtained by the EDP- or IM-based approach, especially, since the equal displacement rule is valid and we have b=1 in Eq. (5b). This confirms the sound basis of both formulations. Still, we expect them to differ more when the power law approximation of Eq. (5b) is no longer accurate, or

when we approach global dynamic instability where the EDP formulation becomes inaccurate (see Vamvatsikos and Dolšek (2009) and references therein). Finally, the selection of the value of the dispersion measure becomes more significant when the value of the hazard curve slope k is high, for example, for the ductile limit state (k=3.5), something that may cause different results in the two formulations.

For the potential brittle limit state the corrosion significantly increases the seismic risk since the corrosion of the shear reinforcement has a relatively greater influence on the shear capacity. This becomes apparent in the static pushover curves, where, consequently, the roof displacement that corresponds to that limit state decreases by about 4.0 mm per decade or 2.2 cm in 50 years. This is a relatively large reduction compared to the initial condition, in which the maximum roof displacement at potential brittle limit state amounts to 5.3 cm. However, this is not true for the case of the NC limit state, since the corrosion of longitudinal reinforcement practically does not have any influence on the calculated ultimate rotations in the plastic hinges. As a result, the maximum roof displacements at the ductile NC limit state for different instants of time decreases by just a few percents, that is 0.9 cm in 50 years (Table 1).

In addition to the averaged results in Tables 4 and 5, the instantaneous MAFs were calculated (Cornell at al. 2002), which via the EDP-based formulation can be estimated as

$$\lambda_{\text{edp}}\ t\ = k_0\ \hat{a}_{\text{g,ls}}(t)^{\ -k} \cdot \exp\left[\frac{k^2}{2b^2}\ \beta_{\text{DR}}^2 + \beta_{\text{CR}}^2 + \beta_{\text{DU}}^2 + \beta_{\text{CU}}^2\ \right], \tag{16}$$

where the seismic intensity measure $\hat{a}_{\text{g,ls}}(t)$ is related to the selected limit state capacity at time t. Such values may be of interest as they represent the MAFs derived by a performance evaluation (based on current probabilistic frameworks) that takes place at that instant in the building's lifetime. Therefore the instantaneous MAFs may heavily influence future rehabilitation decisions. For example, the MAFs of exceedance of the NC and potential brittle limit states for the initial structure using the EDP-based formulation are estimated at 0.0276×10^{-2} and 0.559×10^{-2}, respectively. Otherwise, the corresponding instantaneous return periods are around 3620 and 180 years, respectively. For comparison, the instantaneous return periods for exceedance of the two limit states after 50 years of corrosion propagation decrease to 2930 and 75 years, respectively.

4 CONCLUSIONS

A simplified methodology has been presented for estimating the seismic performance of ageing RC structures. Considering the deterioration of longitudinal and shear reinforcement due to corrosion, and utilizing simplified analysis techniques within a SAC/FEMA-like probabilistic framework, we are able to estimate the changing mean annual frequency (MAF) of limit state exceedance as it worsens with time. Finally, the time-average of the MAF of limit state exceedance is quantified over a continuous time period, providing us with a cumulative single measure of the structure's performance as ageing sets in. Two different approaches were demonstrated to achieve these estimates, based on the EDP and IM formulation of the SAC/FEMA probabilistic framework, the latter being suitable for all limit states, even close to global collapse.

In our case-study of a 3-story non-ductile RC structure, both approaches were shown to produce similar results, as long as we properly assign the values of dispersion, especially, if the hazard curve slope k is relatively steep. Thus, corrosion is shown to have moderate influence on the moment capacity of beams and columns, while their shear capacity was

heavily degraded. However, the later issue is not reflected in the average MAF of violating the NC limit state, since the structure is not sensitive to brittle failure. Therefore, we defined a potential brittle limit state, which indicates shear capacity degradation, and observed around 40 % increase of the average MAF of exceedance events at which the storey shear demand/capacity ratio exceeds 50 %. This is a significant increase that simply cannot be ignored if structures contain shear-critical members, something that tends to be the norm in older RC buildings.

It is envisaged that further refinement of our corrosion model with inclusion of concrete spalling and bond degradation will additionally increase the estimated seismic risk of ageing RC structures. Thus, further verifications of such results are needed in order to better understand the actual risks faced by our ageing infrastructure and appropriately amend our design codes.

ACKNOWLEDGEMENTS

The authors wish to acknowledge the support of the Cyprus Research Promotion Agency under grant CY-SLO/407/04 and of the Slovenian Research Agency under grant BI-CY/09-09-002.

REFERENCES

Berto L, Vitaliani R, Saetta A, Simioni P (2009) Seismic assessment of existing RC structures affected by degradation phenomena. Struct Saf 31: 284-297.

CEN (2004) Eurocode 8: Design of structures for earthquake resistance. Part 1: General rules, seismic actions and rules for buildings, EN 1998-1. European Committee for Standardisation, Brussels, December 2004.

CEN (2005) Eurocode 8: Design of structures for earthquake resistance. Part 3: Strengthening and repair of buildings. EN 1998-3, European Committee for Standardisation, Brussels, March 2005.

Choe D, Gardoni P, Rosowsky D, Haukaas T (2009) Seismic fragility estimates for reinforced concrete bridges subject to corrosion. Struct Saf 31: 275-283.

Cornell CA, Jalayer F, Hamburger RO, Foutch DA (2002) Probabilistic Basis for 2000 SAC Federal Emergency Management Agency Steel Moment Frame Guidelines. J Struct Eng 128: 526-533.

Dolsek M (2009) Development of computing environment for the seismic performance assessment of reinforced concrete frames by using simplified nonlinear models. Bull Earth Eng (in review).

Dolsek M (2009) Incremental Dynamic Analysis with consideration of modeling uncertainties. Earthq Eng Struct Dynam 38: 805-825.

Dolšek M, Fajfar P (2008) The effect of masonry infills on the seismic response of a four storey reinforced concrete frame–a probabilistic assessment. Eng Struct 30:3186-3192.

Dolšek M, Fajfar P (2007) Simplified probabilistic seismic performance assessment of plan-asymmetric buildings. Earthq Eng Struct Dynam 36:2021–2041.

Estes AC, Frangopol DM (2001) Bridge lifetime system reliability under multiple limit states. J Bridge Eng 6(6): 523-528.

Fajfar P (2000) A nonlinear analysis method for performance-based seismic design. Earthq Spec 16(3):573-592.

Fajfar P, Dolšek M, Marušić D, Stratan A (2006) Pre- and post-test mathematical modeling of a plan-asymmetric reinforced concrete frame buildings. Earthq Eng Struct Dynam 35: 1359-1379.

FEMA 350 (2000) Recommended seismic design criteria for new steel moment frame buildings. SAC Joint Venture, Federal Emergency Management Agency, Washington (DC).

FEMA P695 (2009) Quantification of Building Seismic Performance. ATC-63 Projest Report – 90 % Draft, Federal Emergency Management Agency, Washington (DC).

Kumar R, Gardoni P, Sanchez-Silva M (2009) Effect of cumulative seismic damage and corrosion on the life cycle cost of reifirced concrete bridges. Earthq Eng Struct Dynam 38:887–905.

McKenna F, Fenves GL (2004) Open system for earthquake engineering simulation, Pacific Earthquake Engineering Research Center, Berkeley, California. http://opensees.berkeley.edu/

Pantazopoulou SJ, Papoulia KD (2001) Modeling Cover-Cracking due to Reinforcement Corrosion in RC Structures. J Eng Mech 127(4): 342-351.

Peruš I, Poljanšek K, Fajfar P (2006) Flexural deformation capacity of rectangular RC columns determined by the CAE method. Earthq Eng Struct Dynam 35: 1453-1470.

Rozman M, Fajfar P (2009) Seismic response of a RC frame building designed according to old and modern practices. Bull Earthq Eng 7:779-799.

Ruiz-Garcia J, Miranda E (2003) Inelastic displacement ratios for evaluation of existing structures, Earthq Eng Struct Dynam 32:1237-1258.

Stewart MG (2009) Mechanical behavior of pitting corrosion of flexural and shear reinforcement and its effect on structural reliability of corroding RC beams. Struct Saf 31:19-30.

Torres MA, Ruiz SE (2007) Structural reliability evaluation considering capacity degradation over time. Eng Struct 29: 2183-2192.

Val DV, Stewart MG, Melchers RE (1998) Effect of reinforcement corrosion on reliability of highway bridges. Eng Struct 20: 1010-1019.

Val DV, Stewart MG (2009) Reliability assessment of ageing reinforced concrete structures – current situation and future challenges. Struct Eng Inter 19(9): 211-219.

Vamvatsikos D, Dolšek M (2009) Equivalent constant rates for performance-based seismic assessment of ageing structures. Struct Saf (in review).

Vamvatsikos D, Cornell CA (2002) Incremental Dynamic Analysis. Earthq Eng Struct Dynam 31:491-514.

Vamvatsikos D, Cornell CA (2006) Direct estimation of the seismic demand and capacity of oscillators with multi-linear static pushovers through Incremental Dynamic Analysis. Earthq Eng Struct Dynam **35**(9): 1097–1117.

Yun S-Y, Hamburger RO, Cornell CA, Foutch DA (2002) Seismic performance evaluation for steel moment frames. J Struct Eng ASCE 128(4): 534-545.